COMPONENT PART NOTICE

THIS PAPER IS A COMPONENT PART OF THE FOLLOWING COMPILATION REPORT:

TITLE: Target and Clutter Scattering and Their Effects on Military Radar Performance (Diffraction par les Cibles et le Fouillis et ses Effets sur les Performances des Radars Militaires).

TO ORDER THE COMPLETE COMPILATION REPORT, USE AD-A244 893.

THE COMPONENT PART IS PROVIDED HERE TO ALLOW USERS ACCESS TO INDIVIDUALLY AUTHORED SECTIONS OF PROCEEDING, ANNALS, SYMPOSIA, ETC. HOWEVER, THE COMPONENT SHOULD BE CONSIDERED WITHIN THE CONTEXT OF THE OVERALL COMPILATION REPORT AND NOT AS A STAND-ALONE TECHNICAL REPORT.

THE FOLLOWING COMPONENT PART NUMBERS COMPRISE THE COMPILATION REPORT:

AD#: P006 373 thru AD#: P006 396

AD#: AD#:

AD#: AD#:

DTIC FORM 463
MAR 85

OPI: DTIC-TID

STOCHASTIC MODEL OF TERRAIN EFFECTS UPON THE PERFORMANCE OF LAND-BASED RADARS

S P TONKIN
Smith Associates Limited
Guildford Surrey GU2 5YP
UK

M A WOOD
Royal Signals and Radar Establishment
Great Malvern Worcestershire WR14 3PS
UK

Summary

A stochastic model of land clutter visibility and of terrain screening of targets, with particular application to low-flying targets under surveillance by a microwave land-based radar system, is described.

The model is non-site-specific, but detailed. It allows radar performance measures such as the mean length of track to be obtained analytically, without averaging large numbers of site-specific simulations or requiring high fidelity terrain data. The trajectories of terrain-following targets are described in terms of ensembles of Markov processes. The main dependencies of the model are on:

- terrain relief;
- radar height;
- target altitude;
- distance of closest approach between the target and the radar.

The model can be used to generate simulated clutter maps and target screening diagrams, and indeed this is done to compare the model results with experimental data. However, the main aim is to predict the effects of target screening and land clutter directly from the model, rather than through large numbers of simulations. The equations which can be used to derive such predictions are given, and applied to a simple case: the time at which an incoming target first enters a cluttered cell. This approach to such calculations is extremely computationally efficient.

Introduction

In performance assessments of ground based air defence radar systems, the quantity of interest is usually a general measure such as the mean track length. Ultimate limits upon such performance measures are provided by certain characteristics of the terrain: in particular, terrain screening and land clutter. An important feature of these terrain effects is their patchiness: for example, low-flying targets may move in and out of clutter several times while flying towards the radar site. The path of a low-flying air vehicle relative to such terrain features can critically affect the radar performance; this is illustrated in Figure 1.

Figure 1
Illustration of the effect of the path of a low-flying air vehicle on its detectability

Two classes of model have been used to predict such effects. Detailed site-specific models[1] can predict radar performance for a particular radar site and air vehicle trajectory; such models rely on high fidelity terrain and land cover data. However, while the performance for a well-specified site and trajectory can be found, it is not clear how many sites and how many trajectories for each site would have to be analysed to give a statistically significant answer; furthermore, this approach is computationally expensive. In contrast, simplistic spherical-earth clutter and screening models do not address the wide variability of clutter and screening effects with different target paths.

The purpose of this paper is to outline a stochastic model of terrain screening and land clutter, which provides a middle way between the detailed site-specific and simple spherical-earth models. The stochastic model, which has been tested against measured clutter data and digital terrain elevation data (DTED), describes the large-scale spatial correlations of target screening and of clutter for three generic classes of terrain (level, low-relief and high-relief).

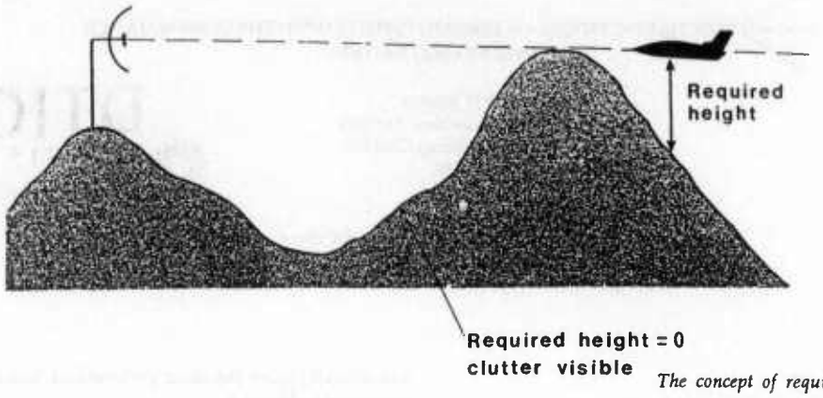

Figure 2
The concept of required height

Terrain-following Targets and Ground Clutter

The screening of terrain following targets can be described in terms of a single quantity, the height, h_r, above the terrain that the target must reach to be visible. The concept of required height is illustrated in Figure 2; the occurrence of (line of sight) ground clutter corresponds to regions where this required height is zero. The required height can be defined at every point within the region of interest, giving:

$$h_r = h_r(R, \theta) \qquad (1)$$

where R and θ are polar coordinates relative to the radar site as origin.

The proposed stochastic model characterises the required height $h_r(R,\theta)$ as a random field, with a different ensemble of such fields corresponding to each of the terrain classes of interest. The terrain classes considered are:

(i) **Level sites**: these are generally well modelled in terms of a spherical earth. At X-band, the clutter visibility, defined as the fraction of cells at a given range which are cluttered, gradually falls away with range, the main drop in clutter visibility occurring near the spherical earth horizon.

(ii) **Low-relief sites** (eg gently rolling farm-land): in these regions, the clutter persists beyond the spherical earth horizon, and there is patchiness, or correlation, in the clutter visibility. An X-band clutter map for such a site, Spruce Home, is given in Figure 3 (upper map). The maximum range in this figure (and all other clutter maps shown here) is 24 km; the "spherical earth" clutter horizon for the given radar height (18 m) is only 16 km.

(iii) **High-relief sites** (ie mountainous areas): here, the clutter persists at very long ranges, and there may be anisotropy and periodicity in the clutter visibility due to regular mountain ridges. The illustrative clutter map shown in Figure 3 (lower map) was measured at Scranton.

Spruce Home (low-relief)

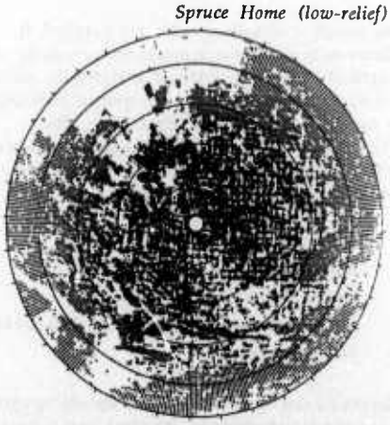

Scranton (high-relief)

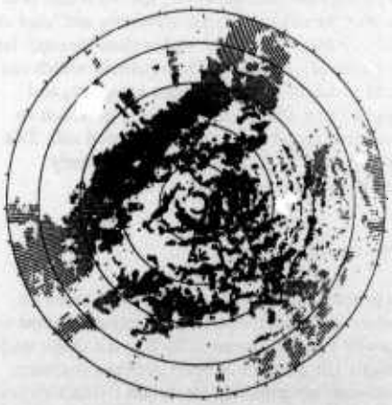

Figure 3
Clutter maps for a low-relief site, Spruce Home, and a high-relief site, Scranton.

A reasonable statistical description of the terrain shadowing is obtained in terms of an underlying random field, $g(R,\theta)$, such that:

$$h_r(R,\theta) = g(R,\theta)^2 \qquad g(R,\theta) > 0 \ ;$$
$$h_r(R,\theta) = 0 \qquad g(R,\theta) \le 0 \ . \qquad (2)$$

The root required height, $\sqrt{h_t(R,\theta)}$, follows a truncated Gaussian distribution characterised by a mean, $\mu(R)$, and a standard deviation, $\sigma(R)$, with the following functional forms:

$$\mu(R) = A + B\,R + C\,h^* \ ;$$
$$\sigma(R) = \sigma \ . \qquad (3)$$

The parameters A, B, C and σ are constant for a given terrain type, and h^* is the height of the radar above the mean terrain height. Figure 4 illustrates this truncated Gaussian distribution for $\sqrt{h_t(R,\theta)}$; histograms of the root required height at different ranges, constructed from a single (low-relief) shadowing diagram, are shown, together with the best fit (maximum likelihood) Gaussian. The spike at zero required height, corresponding to cluttered regions, has been removed.

The two point correlation function of the normal field g can be expressed:

$$\rho(r_0,r_1) = \exp\left\{-\int_{r_0}^{r_1} \alpha(R,\psi,\zeta)\,dr\right\} \ . \qquad (4)$$

The function $\alpha(R,\psi,\zeta)$ is terrain type dependent. The angle ψ describes the direction of the target's path relative to the radial direction (ie ψ=0 implies a radial path and ψ=90° implies a tangential path), and the angle ζ describes the path's direction relative to a fixed direction (this latter dependence only arises in high-relief sites, in which a preferred direction is defined by the mountain ridges).

The model parameters, A, B, C, σ and the function α have been evaluated from DTED corresponding to each of the classes of site. The values given here are tentative, since a sufficiently large data set to give firm values has yet to be analysed.

(i) **Level sites**: as the scattering arises from vertical discretes[1], simulated screening diagrams can be constructed by applying an uncorrelated clutter distribution to a screening diagram for a spherical earth, modelled deterministically. Formally, this gives the following parameterisation (where a_E is the earth radius):

$$\mu(R) = \frac{R - \sqrt{2a_E\,h^*}}{\sqrt{2a_E}} \ ;$$
$$\sigma(R) = 0 \ ;$$
$$\rho(r_1,r_2) = 0 \ . \qquad (4)$$

(ii) **Low-relief sites**: Table 1 gives values for the parameters A, B, C and σ (note that since g is the square root of a height, the units of μ and σ are $\sqrt{}$(metres)). The site height h^* for the particular case considered, Spruce Home, is 37 m. In addition, the two-point correlation function (defined in terms of α) can be written:

$$\alpha(R,\psi,\zeta) = P_0 \exp\left(-\frac{R^2}{R_0^2}\right) + P_1 + Q_\psi \sin\psi + Q_\zeta \sin\zeta \ . \qquad (5)$$

The parameters P_0, P_1, R_0, Q_ψ and Q_ζ are given in Table 2. For low-relief sites, the parameter Q_ζ (describing the dependence of the correlations upon the direction of the path relative to a preferred direction) vanishes, implying that, on average, the screening diagrams are isotropic.

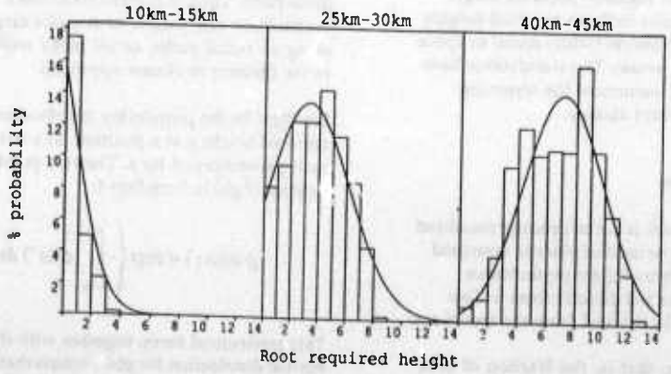

Figure 4
Histograms of the square root of the required height for three different ranges; zero-height values removed

	A/√m	B/m$^{-1/2}$	C/m$^{-1/2}$	σ/√m
Low-relief	-3.6	0.3×10^{-3}	-0.05	3.2
High-relief	+14.7	0.6×10^{-3}	-0.07	6.3

Table 1
Parameters describing the single-point statistics of g

	P_0/km^{-1}	P_1/km^{-1}	R_0/km	Q_ψ/km^{-1}	Q_ζ/km^{-1}
Low-relief	0.25	0.005	40.	0.02	0.0
High-relief	0.20	0.005	20.	0.005	0.02+0.14i

Table 2
Parameters describing the correlations of g

(iii) High-relief sites: clutter visibility and target screening are much more variable for high-relief than for low-relief and level sites. The parameters describing the required height field are given in Tables 1 and 2; Scranton has a site height of 203 m. The most salient feature of this parameter set is the parameter Q_ζ, which is not only non-zero but also complex. Exponentiation of this complex α (as in Eqn 4) gives a periodic correlation; this is needed to describe the periodicity of the ridges illustrated in Figure 3.

Given this complete parameter set, screening diagrams can be simulated for each class of site. Figures 5 and 6 give such simulated screening diagrams, together with a screening diagram generated from DTED, for the low-relief and high-relief terrain types. In these diagrams, the black areas indicate cluttered regions (required height zero), and the grey scales indicate required heights ranging from below 50 metres (white areas) to above 200 metres (dark grey areas). The simulations have captured the essential features of the screening diagrams for the different classes.

Performance Prediction

The purpose of this work is not to produce simulated screening diagrams to be used in place of measured ones; rather, quantities useful for performance prediction can be extracted directly from it. Two quantities which can be derived from the model are:

- clutter visibility, that is, the fraction of cells at a given range that are cluttered;
- the probability that a target is visible and in an uncluttered cell.

For example, the clutter visibility $V(R)$ is:

$$V(R) = \frac{1}{2}\,\mathrm{erfc}\left(\frac{A + B\,R + C\,h^*}{\sigma\sqrt{2}}\right) . \qquad (6)$$

At long ranges, $V(R)$ is proportional to $\exp(-B^2R^2/2\sigma^2)$.

For more detailed predictions, the evolution of the probability distribution function $P(g)$ is used. By describing the way in which $P(g)$ changes along a straight line path defined relative to the radar site, the whole ensemble of equivalent paths can be described at once - at no time is it necessary to consider a number of specific paths and simulate particular values for the required heights along those paths. Thus, it is possible to use a single, probabilistic calculation to describe target detection along all radial paths, or all paths with (say) 10 km as the distance of closest approach.

Let $P(g;s)$ be the probability distribution of the root required height g at a position on a straight-line path parameterised by s. The two-point correlation function of $g(s)$ is, from Eqn 4:

$$\rho(s_0,s_1) = \exp\left\{-\int_{s_0}^{s_1} \alpha(s')\,ds'\right\} . \qquad (7)$$

This exponential form, together with the assumed normal distribution for $g(s)$, means that $g(s)$ is described by a normal Markov process[2].

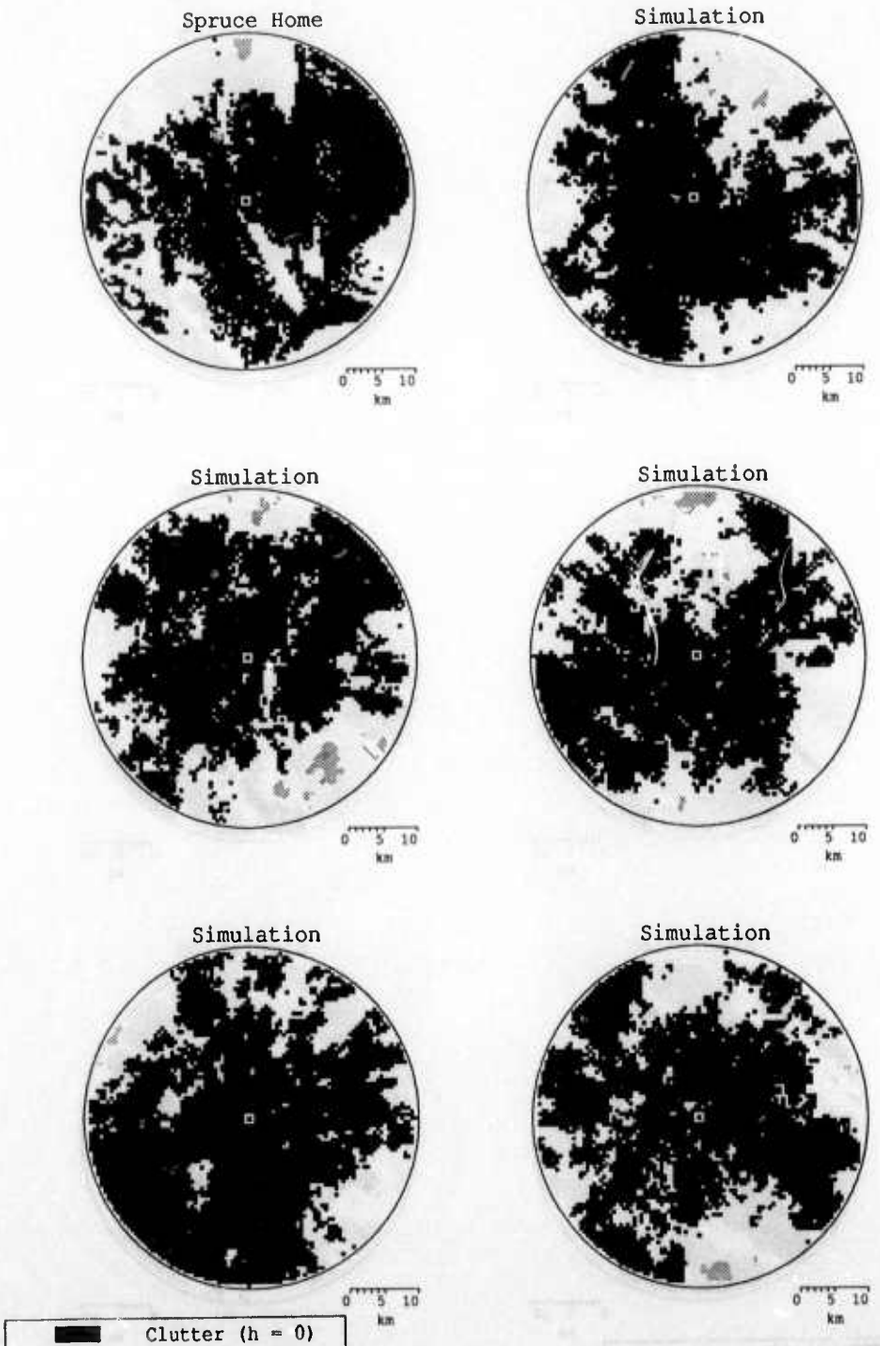

Figure 5
Comparison of a low-relief screening diagram produced using the DTED for Spruce Home (top left-hand corner) with simulations produced using the non-site-specific model

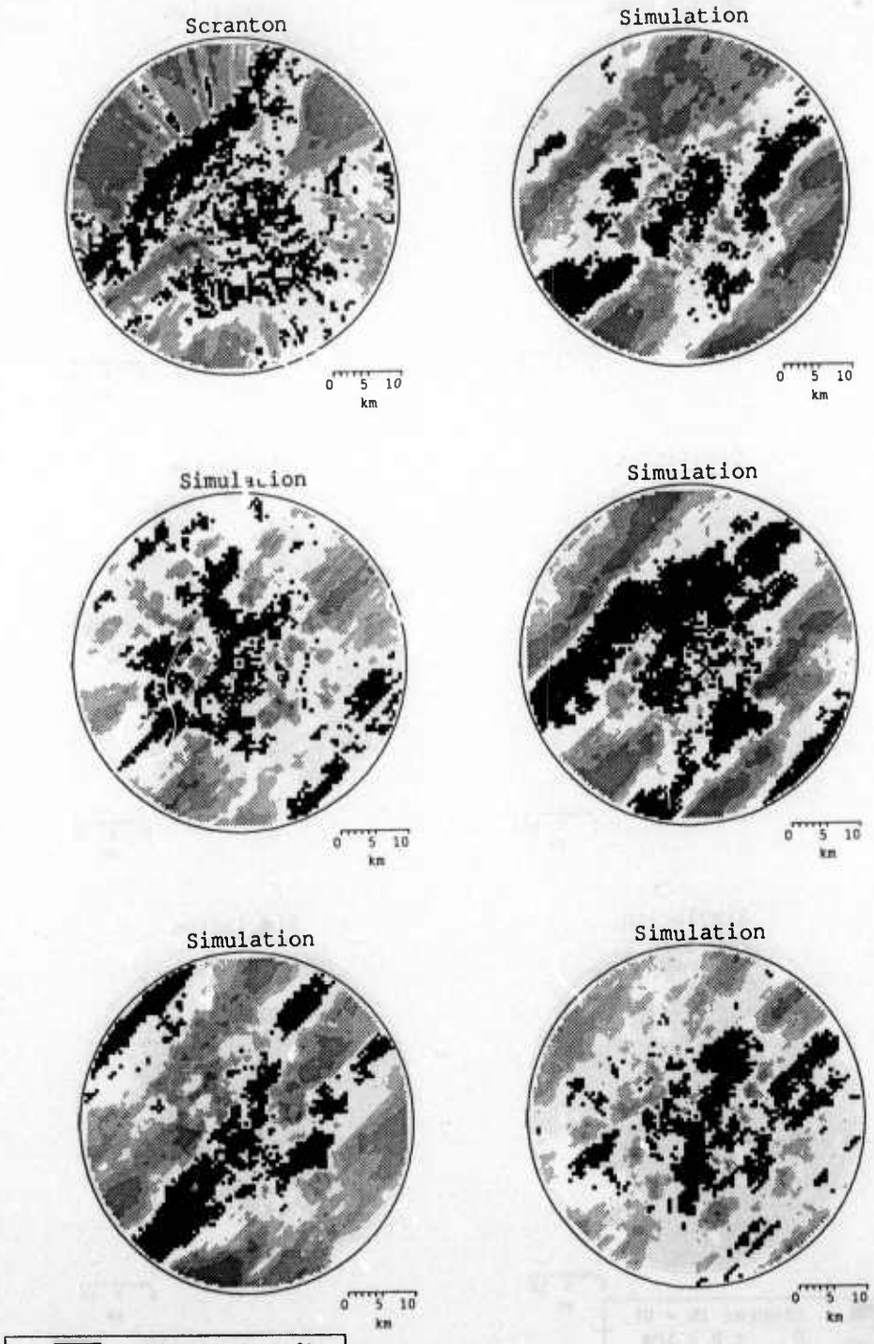

Figure 6
Comparison of a high-relief screening diagram produced using the DTED for Scranton (top left-hand corner) with simulations produced using the non-site-specific model

This in turn means that the probability distribution function for $g(s)$, $P(g;s)$, obeys the (forward) Kolmogorov equation[2]:

$$\frac{\partial P(g;s)}{\partial s} = \alpha(s)\frac{\partial^2 P(g;s)}{\partial g^2} + \left(\alpha(s)[g-\mu(s)] - \frac{d\mu(s)}{ds}\right)\frac{\partial P(g;s)}{\partial g} + \alpha(s)P(g;s) \equiv K_g[P(g;s)] \quad . \tag{8}$$

In this equation, $\alpha(s)$ is the rate of decorrelation at a position s along the path, $\mu(s)$ is the mean value of g at position s, and σ is the (range-independent) standard deviation of g. The quantities α, μ, and σ depend on the range to the radar site, the radar height and the terrain type; the different possible paths are described through the dependence of the range R upon the distance s. For example, for radial paths beginning at range R^0, that range is $(R^0 - s)$. For non-radial paths, the range depends on the distance of closest approach, as well as upon R^0 and s. The operator $K_g[P(g;s)]$ is defined by the right-hand-side of Eqn 8.

Because the Kolmogorov equation is a parabolic partial differential equation, it is easy to solve numerically for a range of boundary conditions[3].

As an example of the use of this equation, consider the problem of the range at which a terrain-following target flying along an incoming radial path, starting at a range R^0, first becomes unshadowed. Suppose that the target flies at a height h_t above the terrain. This means that the target will first become unmasked when the required height for a line of sight first drops below h_t; that is, when the root required height $g(r)$ first drops below $\sqrt{h_t}$. The probability that the target has become unshadowed at or before range R is equal to the probability that $g(r')$ drops below $\sqrt{h_t}$ between $R' = R^0$ and $R' = R$.

To calculate this probability, the Kolmogorov equation is integrated from $R' = R^0$ to $R' = R$. The initial state for $P(g;s)$ is the distribution function for the root required height g at the initial position R^0, $P(g(R^0))$ or $P(g;s=0)$. This is a normal distribution with mean $\mu(R^0)$ and standard deviation σ. By integrating Eqn 8 from this initial state, the distribution of $g(R)$ at any range R (ie any position s along the path) can be found. If the boundary condition

$$P(g \le \sqrt{h_t}\,;s) = 0 \tag{9}$$

is applied, that is equivalent to removing from the distribution function all paths for which the root required height g has dropped below the square root of the target height $\sqrt{h_t}$; the resulting distribution function $P(g;s)$ then refers to that subset of paths in which the root required height g has never passed $\sqrt{h_t}$. Therefore, the probability at any position s that g has never passed $\sqrt{h_t}$ (and consequently the target has never become unscreened) is:

$$P\ (\textit{the target has not yet become visible}) = \int_{\sqrt{h_t}}^{\infty} dg\, P(g;s)\,. \tag{10}$$

Figure 7 illustrates this approach. A number of different curves are shown, indicating the distribution function $P(g)$ at different positions s along the path. The lowest curve illustrates the initial state: g is normally distributed, with a rather high mean value $\mu(s=s_0)$. As the target progresses along the path, the distribution function moves over to the left, until it reaches the boundary at $\sqrt{h_t}$. The boundary condition of Eqn 9 is applied, so that the part of the distribution function which refers to paths which have passed the point $g = \sqrt{h_t}$ has vanished. The probability that a target path has not passed this point is equal to the area under the curve.

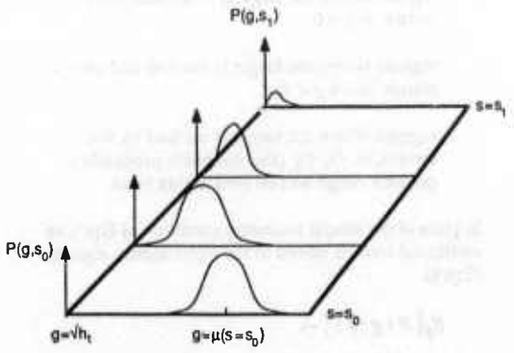

Figure 7
Illustration of the evolution of the probability distribution function P(g;s)

Figure 8 illustrates the results which can be obtained. The curve shows the probability, calculated from the Kolmogorov equation, that an incoming radial target approaching a low-relief site has yet to enter a cluttered cell; that corresponds to setting the target height h_t to zero. The figure also shows the result obtained for the particular site, Spruce Home, by explicitly examining each of 360 radial paths. The curve was very much quicker to obtain computationally (~ 2 seconds cpu time), and it clearly gives similar results to the site-specific case.

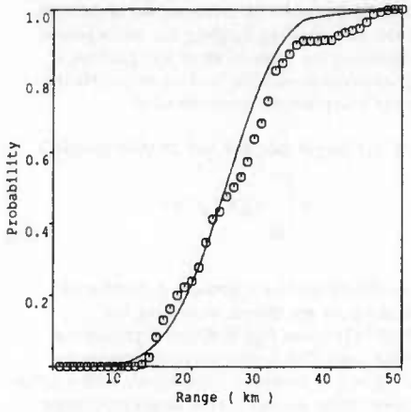

Figure 8
The probability that an incoming radial target has yet to encounter a cluttered cell

A very similar calculation can be used to find the probability that a target at a given range has been detected. Detection probabilities per unit length of path can be defined for:

- regions where the target is unmasked but in clutter, ie $g < 0$;
- regions where the target is masked and clear of clutter, ie $0 \le g < \sqrt{h_t}$;
- regions where the target is masked by the terrain, ie $\sqrt{h_t} \le g$ (the detection probability per unit range will be zero in this case).

In place of the simple boundary condition of Eqn 9, an additional term is added to the Kolmogorov equation (Eqn 8):

$$K_g[\,P(g;s)\,] \rightarrow K_g[\,P(g;s)\,] - p_{det}(g, s, h_t)\,P(g;s) \qquad (11)$$

where p_{det} is the probability per unit length of path that the target is detected (the arguments of p_{det} take into account the three regions just listed). This additional term ensures that the probability that the target is still undetected at a given position on the path drops at the appropriate rate. The simple boundary condition of Eqn 9 corresponded to the following limiting choice of p_{det}:

$$p_{det}(g, s, h_t) = \begin{cases} 0, & g > \sqrt{h_t}\,; \\ \infty, & g \le \sqrt{h_t}\,. \end{cases} \qquad (12)$$

It is just as straightforward to evaluate (for example) the range at which there is a 50% chance that a target has been detected as is it to find the range at which there is a 50% chance that it has been unmasked.

Conclusions

The non-site-specific, stochastic model of land clutter visibility and of terrain screening of targets described in this paper appears to fit the data well. The model accounts for the correlations in target screening and clutter visibility, as well as their mean levels. It makes it possible to answer quite detailed questions (eg concerning the length of track which is likely to be available to a land-based radar system) relating to general classes of sites, with a high degree of computational efficiency.

Acknowledgements

This work has been carried out with the support of the Procurement Executive, Ministry of Defence.

The radar ground clutter measurement data referred to in this paper were collected by Lincoln Laboratory, a centre for research operated by Massachusetts Institute of Technology. This work was sponsored in the United States by the US Defense Advanced Research Projects Agency and the US Department of the Air Force under Air Force Contract F19628-85-C-0002 (ARPA Order 3724). Many of the measurements were conducted in Canada under a Memorandum of Understanding between the US Department of Defense and the Canadian Department of National Defence.

References

1 BILLINGSLEY J B, *'Radar Ground Clutter Measurements and Models, Part 1'*, this conference.

2 PAPOULIS A, *'Probability, Random Variables and Stochastic Processes'*, McGraw-Hill, 1965.

3 *'NAG Fortran Library, Introductory Guide - Mark 13'*, 1988.

DISCUSSION

E. Luneburg, GE

The approaching aircraft follows the natural terrain. Is this accounted for in your modelling?

Author's Reply

The aircraft follows the terrain in the sense that it remains at a constant height above the local terrain (e.g., it goes up when it encounters a hill). The model does not account for the possibility that the aircraft might choose to fly around a hill rather than over it; however, modelling such detailed aspects of the aircraft's trajectory is probably better done in a site-specific framework.